Available online at www.sciencedirect.com
ScienceDirect
Journal of Solid State Chemistry 181 (2008) 1279–1284
JOURNAL OF SOLID STATE CHEMISTRY
www.elsevier.com/locate/jssc

Hydrothermal synthesis, characterization and fluorescence property of a novel layered fluorinated gallium phosphite with heptameric building unit

Liangliang Huang, Tianyou Song, Suhua Shi, Zhenfen Tian, Li Wang*, Lirong Zhang*

College of Chemistry, Jilin University, Changchun 130012, China

Received 17 December 2007; received in revised form 28 January 2008; accepted 31 January 2008
Available online 9 February 2008

Abstract

A new fluorinated gallium phosphite, $Ga_3F_2(2,2'\text{-bipy})_2(HPO_3)_2(H_{1.5}PO_3)_2$ **1**, which is the first layered gallium phosphite with neutral framework, has been hydrothermally synthesized in the presence of 2,2′-bipyridine (2,2′-bipy) acting as a ligand. The as-synthesized product was characterized by single-crystal X-ray diffraction, powder X-ray diffraction, IR spectroscopy, thermogravimetric analysis (TGA), ICP-AES and elemental analyses and fluorescent spectrum. Single-crystal X-ray diffraction analysis reveals that compound **1** crystallizes in the monoclinic space group $C2/c$ (No. 15) with cell parameters $a = 17.633(3)$ Å, $b = 9.883(2)$ Å, $c = 16.793(3)$ Å, $\beta = 109.88(3)^\circ$, $V = 2752.1(9)$ Å^3 and $Z = 4$. The construction of two-dimensional (2D)-layered structure in compound **1** may be viewed as the assembly of heptameric building unit, which is the first to be found in gallium phosphate/phosphite. The heptameric building unit exists in two types of configuration, which alternately connect through oxygen atoms from HPO_3 pseudo-pyramids to form a layer with 10-membered ring windows viewed along the a-axis. The adjacent layers are stably packed together and exhibit interesting three-dimensional (3D) supramolecular array via π–π interactions of the 2,2′-bipy groups. Additionally, compound **1** shows strong fluorescent property in solid state at room temperature.

Keywords: Gallium phosphite; Hydrothermal synthesis; Crystal structure; Fluorescence

1. Introduction

The research of microporous materials with various architectures is of great interest because of their widespread applications in the fields of catalysis, gas storage, separation, adsorption and photochemistry [1]. Following the discovery of aluminophosphate molecular sieves in 1982, a great deal of attention has been paid to the synthesis of open-framework metal phosphates. In recent years, a new change in the synthesis of phosphorus-based microporous materials focuses on the incorporating of pseudo-pyramidal hydrogen phosphite group HPO_3^{2-} in place of tetrahedral phosphate group PO_4^{3-} as the basic building unit and a lot of transition metal phosphites have been prepared hydro- or solvothermally under mild conditions by using organic amines as structure-directing agents or templates [2–6]. However, there are few reports of main block metal phosphites containing organic templates, for example, aluminophosphites, $Al_7(HPO_3)_9(OH)_6 \cdot (C_6H_{12}N_2H_6)_{1.5}(H_2O)_{12}$ [7], $[NH_2(CH_2)_6NH_2][Al(OH)(H(HPO_3))_2]$ [8] and $(H_4bape)_{0.5}[Al(OH)(HPO_3)_2]$ [9]; indium phosphites, $(C_2N_2H_{10})[In(OH)_3(HPO_3)]$ and $(C_4N_2H_{12})[In_2(HPO_3)_3(H_2PO_3)_2]$ [10]. Therefore, we choose to synthesize main block metal phosphite in mild hydrothermal condition as our goal. In our previous work, two gallium phosphites with three-dimensional (3D) open framework, $Ga_3(HPO_3)_4F_4(H_3DETA)$ [11] and $(C_4N_2H_{12})[Ga_2F_3(HPO_3)_2(H_2PO_3)]$ [12], templated by diethylenetriamine (DETA) and piperazine, respectively, have been synthesized and characterized in hydrothermal condition. A study of the literature of the microporous materials shows that 2,2′-bipy not only is a versatile organic ligand to construct appealing architecture of varying dimensions but also shows different

*Corresponding authors. Fax: +86 431 85671974.
E-mail address: lwang99@jlu.edu.cn (L. Wang).

0022-4596/$ - see front matter © 2008 Elsevier Inc. All rights reserved.
doi:10.1016/j.jssc.2008.01.040

photoluminescence property [13,14]; thus, we choose 2,2′-bipy as ligand to synthesize new microporous gallium phosphite. As part of continuing work in Ga-H_3PO_3-amine system, a new 2D layered fluorinated gallium phosphite, Ga_3F_2(2,2′-bipy)$_2$$(HPO_3)_2(H_{1.5}PO_3)_2$ **1**, is synthesized. To our knowledge, it is the first 2D-layered gallium phosphite with organic amine acting as ligand and the structure of layer is constituted by a novel secondary building unit (SBU), the heptamer $Ga_3F_2N_4(HPO_3)_2(H_{1.5}PO_3)_2$, which is never observed in gallium phosphate/phosphite. Herein, we describe the synthesis, crystal structure and characterization of compound **1** along with its fluorescent property.

2. Experimental section

2.1. Materials and instrumentation

All chemicals were obtained from commercial sources and used without further purification. Powder X-ray diffraction (XRD) data were obtained using SHIMADA-ZU XRD-6000 diffractometer with Cu$K\alpha$ radiation ($\lambda=$ 1.5418 Å), with the step size and the count time of 0.02° and 4 s, respectively. The elemental analysis was conducted on a Perkin Elmer 2400 elemental analyzer. ICP-AES (inductively coupled plasma-atomic emission spectroscope) analysis was performed on a Perkin Elmer Optima 3300DV ICP instrument. FT-IR spectrum was recorded on a Nicolet Impact 410 spectrometer between 400 and 4000 cm^{-1} using the KBr pellet method. Thermogravimetric analysis (TGA) was conducted on a Perkin-Elmer TGA 7 thermogravimetric analyzer with a heating rate of 10 °C min^{-1} under flowing nitrogen gas up to 1000 °C. The fluorescence measurement was performed on a Hitachi F-4500 spectrophotometer equipped with a 150 W xenon lamp as the excitation source.

2.2. Synthesis

To a solution of 0.05 g Ga_2O_3 in 6 mL H_2O, was added 0.4 g H_3PO_3 and 0.2 g 2,2′-bipy with stirring, followed by the addition of 0.2 mL HF. The molar composition of the initial mixture was Ga_2O_3:H_3PO_3:2,2′-bipy:HF:$H_2O=$ 1:18:5:18:1028. The mixture was further stirred for 30 min at room temperature and heated at 160 °C for 3 days in a Teflon-lined stainless steel autoclave (filled up to 30% volume capacity) under autogenous pressure, followed by slow cooling down to the ambient temperature. Colorless block-shaped crystals of compound **1** were collected by filtration, washed with distilled water and air-dried. The yield of product was 61% in weight based on gallium.

2.3. Crystal structure determination

A block single crystal with dimensions of 0.10 mm × 0.10 mm × 0.10 mm was carefully selected under a microscope and was mounted inside a glass fiber capillary. The intensity data were collected on a Simens SMART CCD diffractometer with graphite-monochromated Mo$K\alpha$ ($\lambda=$ 0.71073 Å) radiation at a temperature of 293(2) K. No significant decay was observed during the data collection. Data processing was accomplished with the saint-processing program. The structure was solved by direct method using the SHELXTL crystallographic software package [15,16]. The gallium and phosphorus atoms were first located, whereas the carbon, nitrogen, oxygen and fluorine atoms were found in the difference Fourier maps. All the H atoms attached to the carbon were placed geometrically, and the remaining H atoms in the P–H and O–H groups in the compound were located in the difference Fourier maps.

Crystallographic data for compound **1** is listed in Table 1, while the selected bond lengths/angles data are presented in Table 2. CCDC-670935 contains the supplementary crystallographic data for this paper. These data can be obtained free of charge at www.ccdc.cam.ac.uk [or from the Cambridge Crystallographic Data Centre, 12 Union Road, Cambridge CB2 1EZ, UK; Fax: +44 1223/336 033; E-mail: deposit@ccdc.cam.ac.uk].

3. Results and discussion

3.1. Characterizations

The diffraction peaks of powder XRD pattern and the simulated one on the basis of the single-crystal structure analysis are consistent well, indicating the crystal phase

Table 1
Crystal data and structure refinement for compound **1**

Empirical formula	$C_{20}H_{21}F_2Ga_3N_4O_{12}P_4$
Formula weight	880.45
Temperature (K)	293(2)
Wavelength (Å)	0.71073
Crystal system	Monoclinic
Space group	$C2/c$
a (Å)	17.633(3)
b (Å)	9.883(2)
c (Å)	16.793(3)
β (deg)	109.88(3)
V (Å^3)	2752.1(9)
Z	4
μ (mm^{-1})	3.235
F(000)	1744
Theta range for data collection (deg)	3.20–27.43
Limiting indices	$-19\leqslant h\leqslant 22$, $-12\leqslant k\leqslant 12$, $-21\leqslant l\leqslant 21$
Reflections collected/unique	13100/3128 [$R_{int}=0.0694$]
Completeness to theta = 27.43	99.5%
Refinement method	Full-matrix least squares on F^2
Data/restraints/parameters	3128/0/224
Goodness-of-fit on F^2	1.068
Final R indices [$I>2$sigma(I)]	$R_1=0.0445$, w$R_2=0.0765$
R indices (all data)	$R_1=0.0618$, w$R_2=0.0812$
Largest diff. peak and hole (e·Å^{-3})	1.134 and −0.793

$R_1=\sum\|F_o|-|F_{cs}\|/\sum|F_o|$, w$R_2=\sum[w(F_o^2-F_c^2)^2]/\sum[w(F_o^2)^2]^{1/2}$.

Table 2
Selected bond lengths (Å) and angles (deg) for compound **1**

Ga(1)–F(1)	1.995(2)	Ga(1)–O(1)	1.922(3)
Ga(1)–O(2)[a]	1.920(3)	Ga(1)–N(1)	2.093(3)
Ga(1)–O(3)	1.921(3)	Ga(1)–N(2)	2.081(4)
Ga(2)–O(4)	1.972(3)	Ga(2)–O(6)	1.922(3)
Ga(2)–F(1)	1.942(2)	P(1)–O(1)	1.528(3)
P(1)–O(2)	1.504(3)	P(1)–O(6)	1.525(3)
P(1)–H(2)	1.28(4)	P(2)–O(3)	1.523(3)
P(2)–O(4)	1.515(3)	P(2)–O(5)	1.525(3)
P(2)–H(1)	1.38(4)		
Ga(2)–F(1)–Ga(1)	132.79(12)	O(2)[a]–Ga(1)–N(1)	87.73(14)
O(3)–Ga(1)–N(1)	169.89(14)	O(2)[a]–Ga(1)–N(2)	90.18(13)
O(1)–Ga(1)–N(1)	93.00(13)	O(3)–Ga(1)–N(2)	92.15(14)
F(1)–Ga(1)–N(1)	87.83(12)	O(1)–Ga(1)–N(2)	169.47(13)
N(2)–Ga(1)–N(1)	77.89(14)	F(1)–Ga(1)–N(2)	85.06(12)
P(1)–O(1)–Ga(1)	133.84(17)	P(2)–O(3)–Ga(1)	128.67(18)
P(1)–O(2)–Ga(1)[b]	139.3(2)	P(1)–O(6)–Ga(2)	133.65(19)
P(2)–O(4)–Ga(2)	129.12(18)	P(2)–O(5)–H(5)	115(3)
O(2)–P(1)–H(2)	106(2)	O(4)–P(2)–H(1)	112.3(17)
O(6)–P(1)–H(2)	107(2)	O(3)–P(2)–H(1)	107.7(17)
O(1)–P(1)–H(2)	108(2)	O(5)–P(2)–H(1)	101.8(17)

Symmetry transformations used to generate equivalent atoms:
[a] $-x+1/2,\ y+1/2,\ -z+1/2$;
[b] $-x+1/2,\ y-1/2,\ -z+1/2$.

purity of the as-synthesized samples. The ICP and elemental analysis results are listed as follows: anal. found: Ga, 23.71%; P, 13.93%; C, 27.14%; H, 2.62%; N, 12.82%. calcd.: Ga, 23.76%; P, 14.07%; C, 27.28%; H, 2.41%; N, 12.71%. F^- content was determined using a fluoride-ion-selective electrode after mineralization and analysis data (exp. 4.24%) is in good agreement with the value (calcd. 4.32%) deduced from the single-crystal XRD analysis.

IR spectrum of the sample showed the stretching vibrations of O–H and C–H bands at 3423, 3129 and 3034 cm^{-1}, and the bands at 1601, 1564, 1493, 1474, 1448 and 1314 cm^{-1} were assigned to the pyridine ring stretching vibrations. The bands at 1171, 1099, 1039 and 923 cm^{-1} were cased by the stretching vibrations of P–O bonds. Both of P–H stretching bands at 2393 and 2416 cm^{-1} indicate the presence of two crystallographically independent phosphite groups in the structure.

TGA was conducted under nitrogen gas with a heating rate of 10 °C min^{-1} from 25 to 1000 °C. The TG curve shows two stages of weight loss between 250 and 900 °C, which can be assigned to the departure of the dehydration (calcd. 5.11 wt% for 2.5 water molecules per formula unit) and 2,2′-bipy ligand (calcd. 35.44 wt% weight loss for two 2,2′-bipy molecule/formula unit). However, the observed total weight loss (33.11 wt%) was much lower than the expected value. The lower reduction in this stage was due to the retention of carbon in the solid residue (black in color). The same phenomenon was observed in GaPOs and InPOs systems [13,17]. Powder XRD measurement for the final product shows that the structure collapses and an unidentified phase is formed.

3.2. Structural description

The asymmetric unit of compound **1** contains 27 independent nonhydrogen atoms, including two gallium atoms, two phosphorus atoms, nine oxygen atoms, two fluorine atoms, ten carbon atoms and two nitrogen atoms, as shown in Fig. 1. All gallium atoms adopt six-coordination geometry, but the coordination environments are different. For Ga(1), it is coordinated three bridging oxygen atoms (O(1), O(3) and O(2A)) from the adjacent P atoms with the average bond length distance 1.921 Å, two nitrogen atoms from a 2,2′-bipy ligand [Ga(1)–N(1): 2.093(3) Å, Ga(1)–N(2): 2.081(4) Å], and one bridging fluorine atom F(1) with the other gallium atom Ga(2) with the bond length distance 1.995(2) Å, which is longer than Ga–O bond length. Ga(2) also shares four bridging oxygen atoms (O(4), O(4A), O(6) and O(6A)) with adjacent P atoms [Ga(2)–O(4): 1.972(3) Å, Ga(2)–O(6): 1.922(3) Å], respectively, except for two bridging fluorine atoms [Ga(2)–F(1): 1.942(2) Å]. All P atoms adopt pseudo-pyramidal coordination geometry, and each bonds to three oxygen atoms and one hydrogen atom. All oxygen atoms bridge to the Ga atoms with the exception of one O(5) atom. In fact, the H peak of electron density is found between the two O(5) atoms and is shared by two $H_{0.5}P(2)O_3$ groups on the adjacent layers, the site occupation factor (SOF) of which is 0.5 for charge balance. Furthermore, the short distance in O(5)–O(5) (2.47 Å) implies that a symmetric H bond O(5)–H–O(5) may exist. Similar behavior has ever been observed in metal phosphates [13,18–20]. The terminal P–H bond lengths are in the range of 1.28(4)–1.38(4) Å, which are similar to the P–H bond length reported in metal phosphites previously [12]. The existence of P–H bond is also verified by the IR

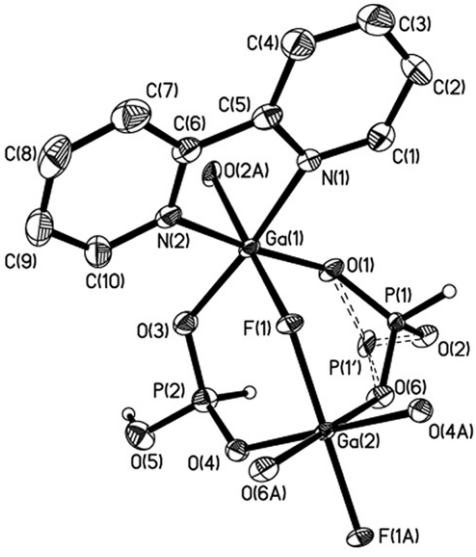

Fig. 1. ORTEP view of the coordination environments of the gallium and phosphorus atoms in compound **1**, showing the labeling scheme and the 50% probability displacement ellipsoids; atom labels with "A" refer to symmetry-generated atoms.

spectrum [21]. The observed bond lengths and angles of compound **1** are in general agreement with those reported in the literature.

The structure of compound **1** consists of infinite neutral layers with 10-membered ring windows. The neutral layer is built up with an unusual SBU, the heptamer $Ga_3F_2N_4(HPO_3)_2(H_{1.5}PO_3)_2$, which consists of two HPO_3 and two $H_{1.5}PO_3$ pseudo-pyramids, two $GaFO_3N_2$ octahedra and a central GaF_2O_4 octahedron. As shown in Fig. 2(a), within the heptameric building unit, the two $GaFO_3N_2$ octahedra and a central GaF_2O_4 octahedron are linked together by the bridging F atoms in *trans*- position to form a trimer $Ga_3F_2O_{10}N_2$. Two HPO_3 and two $H_{1.5}PO_3$ pseudo-pyramids then cap the trimer in *trans*-position by the bridging oxygen atoms to generate a novel heptamer $Ga_3F_2N_4(HPO_3)_2(H_{1.5}PO_3)_2$. There are two types of configuration as shown in Fig. 2(b), named them with I and II in this paper, both of which alternately connect through corner-sharing oxygen atoms from HPO_3 pseudo-pyramids to form a layer with 10-membered ring windows in the *bc* plane (Fig. 2(c)). Interestingly, the adjacent 10-membered ring windows are dissimilar, which can be assigned to the two types of configuration of heptamer. The adjacent inorganic layers are stacked in an AAAA sequence along the *a*-axis, as shown in Fig. 3, 2,2′-bipy ligands decorate the inorganic layer and project above and below into the interlamellar regions. The neighboring 2,2′-bipyridine ligands from two adjacent two-dimensional (2D) layers are almost parallel to each other, and there are possible π–π stacking interactions between them as reflected in an average distance of 3.42 Å. Therefore, the 2D layers of compound **1** are further extended into a 3D supramolecular array via the zipper-like intercalation of the lateral aromatic groups. It is noted that there are no H-bonds between the adjacent layers.

Fluoride method has proved to be an effective and promising method in promoting synthesis of large zeolite single crystals, aluminosilicates and new metal phosphates especial in gallium phosphates. By introducing fluoride into the synthetic system of gallium phosphates [22–31], F^- acting as a mineralizer may enter in inorganic framework to favor the formation of new framework structure and hitherto several novel structural fragments or secondary building units including fluoride, such as tetramer, pentamer, hexamer, octamer (D4R) and enneamer, have been isolated as shown in Fig. 4. Moreover, in gallium phosphites, only a pentameric building unit has been reported. Therefore, the presence of novel heptameric building unit in the structure of compound **1** is noteworthy, it is the first observed in both gallium phosphates and gallium phosphites. To date, only one similar heptameric building unit has been reported in indium phosphate $In_3F_2(bipy)_2(HPO_4)_3(H_2PO_4)$ [13]. Moreover, although the SBU is similar, the crystal structure between indium phosphate and compound **1** is absolutely different. In the structure of indium phosphate $In_3F_2(bipy)_2(HPO_4)_3(H_2PO_4)$, the heptamers display only one type of configuration and were further linked together via vertex O(4) of the HPO_4 group to form the infinite neutral chains. Whereas in compound **1**, two types of configuration of the heptamer, I and II, alternately connect through corner-sharing oxygen atoms from HPO_3 pseudo-pyramids to form 2D layer with 10-membered ring windows. It may be due to the particular geometry of phosphite and the lower

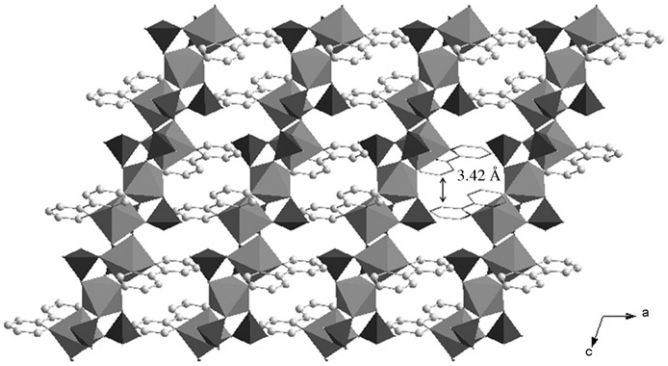

Fig. 3. Polyhedral view of the packing of layers along [010] direction.

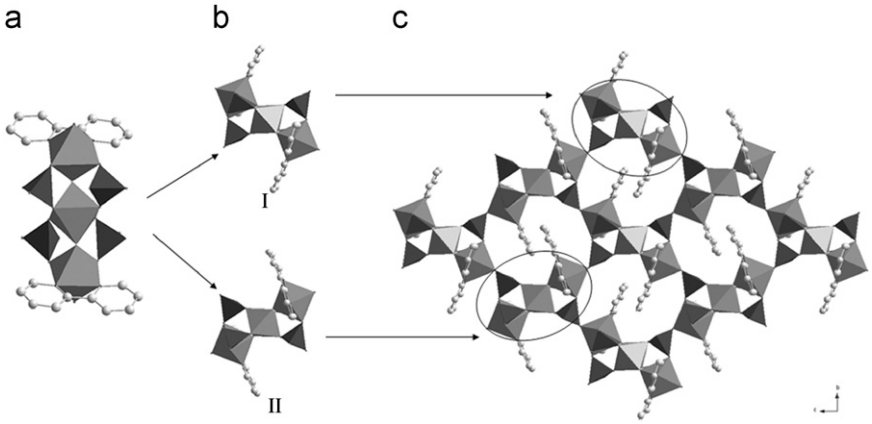

Fig. 2. Description of the structural fashion of compound **1**: (a) The SBU $Ga_3F_2N_4(HPO_3)_2(H_{1.5}PO_3)_2$; (b) two types of configuration I and II; (c) view of the layered structure of compound **1** showing two types of 10-membered ring windows along [100] direction. Key: gray balls C; gray octahedra GaF_2O_4 and $GaFO_3N_2$; black tetrahedra HPO_3.

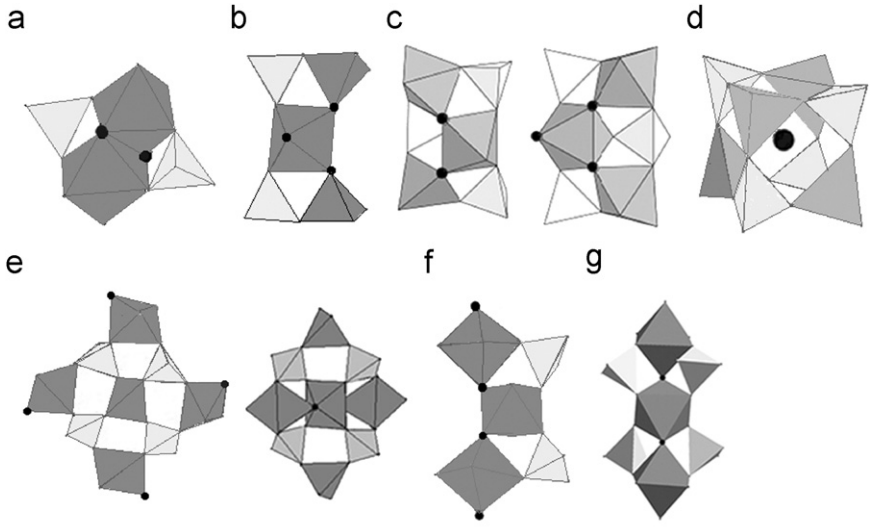

Fig. 4. The SBUs of fluorinated gallium phosphates/phosphites: (a) tetramer $Ga_2(PO_4)_2O_4F_2$; (b) pentamer $Ga_3(PO_4)_2O_3F_2$; (c) hexamer $Ga_3(PO_4)_3O_5F_2$ and $Ga_3(PO_4)_3O_4F_3$; (d) octamer (D4R) $Ga_4(PO_4)_4O_4F$; (e) enneamer $Ga_5(PO_4)_4O_8F_4$ and $Ga_5(PO_4)_4O_4F_2$); (f) pentamer $Ga_3(HPO_3)O_8F_4$ and (g) heptamer $Ga_3F_2N_4(HPO_3)_2(H_{1.5}PO_3)_2$. Key: black polyhedran GaF_4O_2, GaF_3O_3, GaF_2O_4, $GaFO_4$, $GaFO_3$, GaO_4 and $GaFO_3N_2$; gray polyhedran PO_4 and HPO_3; black balls F.

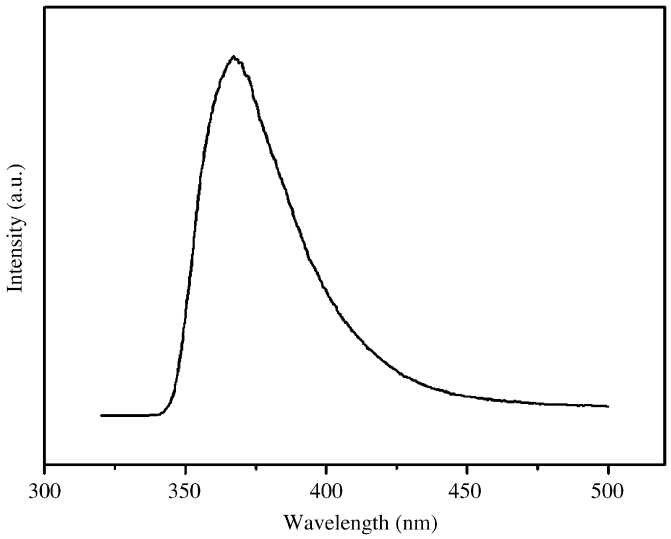

Fig. 5. Solid-state fluorescent emission spectrum of compound **1** ($\lambda_{ex} = 367$ nm) at room temperature.

oxidation states of phosphorous atom. The pyramidal hydrogen phosphite group [HPO_3^{2-}], different from phosphate [PO_4^{3-}], only links three adjacent cations via P–O–M (M = metal) bonds, so it provides variety and novelty to the structures. The oxidation states of phosphorous atoms may directly influence the reactivity of secondary coordination oxygen atoms with adjacent metals.

3.3. Fluorescent spectroscopy

The fluorescent spectroscopy of compound **1** was measured and the solid-state emission spectra at room temperature are shown in Fig. 5. When illuminated with a wavelength of 280 nm, compound **1** displays a strong fluorescence emission band centered at 367 nm, the emission can be assigned as ligand-centered π–π^* transitions [13].

4. Conclusions

In summary, employing 2,2′-bipy as organic ligand, a new fluorinated gallium phosphite with neutral layered framework has been synthesized hydrothermally. The layer structure consists of a novel second building unit, the heptamer, which is the first to be found in gallium phosphate and gallium phosphite. The heptameric building unit exists in two types of configuration, which alternately connect through oxygen atoms from HPO_3 pseudo-pyramids to form a layer with 10-membered ring windows viewed along the *a*-axis. The adjacent layers are stably packed together and exhibit interesting 3D supramolecular array via π–π interactions of the 2,2′-bipy groups. Recently, the pseudo-pyramidal phosphite group, HPO_3, has been investigated as a possible replacement for the traditional phosphate tetrahedron with great success. However, metal phosphites containing organic components coordinated directly to metal atoms are scarce, as compared with the large number of metal phosphites in literature in which the organic components mostly occur as charge compensating and space-filling constituents. Importantly, the photoluminescence property of the compound gives us an approach for obtaining solid-state photoluminescence-emitting materials by the decorating organic ligand. Our investigation shows that it is possible to prepare gallium phosphites with different frameworks or dimensions under appropriate reaction conditions. Further investigation of gallium phosphite is in progress.

Appendix A. Supplementary data

Supplementary data associated with this article can be found in the online version at doi:10.1016/j.jssc.2008.01.040.

References

[1] A.K. Cheetham, G. Férey, T. Loiseau, Angew. Chem. Int. Ed. 38 (1999) 3268.
[2] J. Liang, J.Y. Li, J.H. Yu, P. Chen, Q.R. Fang, F.X. Sun, R.R. Xu, Angew. Chem. Int. Ed. 45 (2006) 2546.
[3] Z. Shi, G.H. Li, D. Zhang, J. Hua, S.H. Feng, Inorg. Chem. 42 (2003) 2357.
[4] S. Fernández, J.L. Mesa, J.L. Pizarro, L. Lezama, M.I. Arriortua, R. Olazcuaga, T. Rojo, Chem. Mater. 12 (2000) 2092.
[5] S. Fernández, J.L. Mesa, J.L. Pizarro, L. Lezama, M.I. Arriortua, T. Rojo, Chem. Mater. 14 (2002) 2300.
[6] J. Fan, G.T. Yee, G.B. Wang, B.E. Hanson, Inorg. Chem. 45 (2006) 599.
[7] A.L. Lu, H.B. Song, N. Li, S.H. Xiang, N.J. Guan, H.G. Wang, Chem. Mater. 19 (2007) 4142.
[8] N. Li, S.H. Xiang, J. Mater. Chem. 12 (2002) 1397.
[9] Y. Xiang, L.W. Zhang, W.H. Chen, J.Z. Chen, Q.X. Zeng, Z. Anorg. Allg. Chem. 633 (2007) 1727.
[10] L. Wang, T.Y. Song, J.N. Xu, Y. Wang, Z.F. Tian, S.H. Shi, Microporous Mesoporous Mater. 96 (2006) 287.
[11] L. Wang, T.Y. Song, Y. Fan, Y. Wang, J.N. Xu, S.H. Shi, T. Zhu, J. Solid State Chem. 179 (2006) 824.
[12] L. Wang, T.Y. Song, Y. Fan, Z.F. Tian, Y. Wang, S.H. Shi, J.N. Xu, J. Solid State Chem. 179 (2006) 3400.
[13] C. Chen, Y.L. Liu, S.H. Wang, G.H. Li, M.H. Bi, Z. Yi, W.Q. Pang, Chem. Mater. 18 (2006) 2950.
[14] Z.E. Lin, J. Zhang, S.T. Zheng, G.Y. Yang, Inorg. Chem. Commun. 6 (2003) 1035.
[15] G.M. Sheldrick, SHELXTL-NT, Version 5.1, Bruker AXS Inc., Madison, WI, 1997.
[16] D.T. Cromer, J.T. Waber, International Tables for X-ray Crystallography, vol. 4, Kynoch Press, Birmingham, AL, 1974 Table 2.2A.
[17] Z.E. Lin, J. Zhang, Y.Q. Sun, G.Y. Yang, Inorg. Chem. 43 (2004) 797.
[18] H.H.-Y. Sung, J.H. Yu, I.D. Williams, J. Solid State Chem. 140 (1998) 46.
[19] C.Y. Chen, F.R. Lo, H.M. Kao, K.H. Lii, Chem. Commun. 12 (2000) 1061.
[20] W.K. Chang, C.S. Wur, S.L. Wang, R.K. Chiang, Inorg. Chem. 45 (2006) 6622.
[21] L. Wang, H. Ding, Y. Hou, L.L. Zhu, Z. Shi, S.H. Feng, J. Solid State Chem. 179 (2006) 2584.
[22] C.H. Lin, S.L. Wang, K.H. Lii, J. Am. Chem. Soc. 123 (2001) 4649.
[23] T. Loiseau, G. Férey, Microporous Mesoporous Mater. 35–36 (2000) 609.
[24] D.S. Wragg, I. Bull, G.B. Hix, R.E. Morris, Chem. Commun. 20 (1999) 2037.
[25] C. Sassoye, J. Marrot, T. Loiseau, G. Férey, Chem. Mater. 14 (2002) 1340.
[26] L. Beitone, J. Marrot, T. Loiseau, G. Férey, M. Henry, C. Huguenard, A. Gansmuller, F. Taulelle, J. Am. Chem. Soc. 125 (2003) 1912.
[27] T. Loiseau, G. Férey, J. Mater. Chem. 6 (1996) 1073 and references cited therein.
[28] T. Loiseau, G. Férey, J. Solid State Chem. 111 (1994) 403.
[29] D.S. Wragg, G.B. Hix, R.E. Morris, J. Am. Chem. Soc. 120 (1998) 6822.
[30] F. Serpaggi, T. Loiseau, F. Taulelle, G. Férey, Microporous Mesoporous Mater. 20 (1998) 197.
[31] Y.L. Yang, Z.C. Mu, Y. Xu, Y.L. Liu, C. Chen, W. Wang, Z. Yi, L. Ye, W.Q. Pang, Solid State Sci. 7 (2005) 103.